

# Femtosecond Laser Drilling of High-Density Micro-Holes on Metals Using MHz Burst Mode

Themistoklis Karkantonis<sup>\*1</sup>, Etienne Pelletier<sup>1</sup>, David Grant<sup>1</sup>, and Dimitris Karnakis<sup>1</sup>

<sup>1</sup> Oxford Lasers Ltd, Unit 8 Moorbrook Park, Didcot OX11 7HP, United Kingdom

<sup>\*</sup>Corresponding author's e-mail: themis.karkantonis@oxfordlasers.com

The pressing need from various technological sectors, e.g. aerospace, automotive and microfiltration, for higher drilling throughput at increasingly lower cost has propelled the continuous commercial development of ultrashort lasers offering very high average powers. Although such laser sources provide a huge potential for production upscaling, it is still challenging to fully utilise their output. The problem relates to unwanted thermal effects that degrade the overall process performance, especially in laser drilling of metal foils. Therefore, effective solutions are still required to exploit these new advances in ultrashort laser technology. Herein, we study throughput upscaling by utilising a 120 W femtosecond diode-pumped solid-state laser in both single-pulse and MHz burst modes for percussion drilling of 300  $\mu\text{m}$  thick stainless-steel foils. The influence of critical laser processing parameters was investigated for maximum drilling efficiency and best hole quality. Heat accumulation effects induced by MHz burst mode in high-density hole drilling were analysed and compared with those of nanosecond laser pulses of similar total temporal length. The results demonstrate new capability using MHz burst mode processing to improve drill rate and hole quality compared to single-pulse. Despite that, MHz burst mode showed similar heat-related issues with a nanosecond laser in high-density drilling operations.

DOI: 10.2961/jlmn.2024.03.2011

**Keywords:** ultrashort laser, percussion drilling, heat accumulation, burst mode, high-throughput

## 1. Introduction

Micro-holes have an essential role in the function of numerous metallic components used in aerospace, automotive, filtration and textile industries [1,2]. To overcome the inherent limitations of traditional microdrilling processes, various non-conventional chipless ones have been developed and deployed to fabricate such holes even in “difficult-to-cut” materials [3]. Among them, laser micro-machining technology has gained a lot of interest from both industrial and academic communities since it offers high processing efficiency, selectivity and flexibility without involving hazardous chemicals [4].

Over the last decade, laser drilling with ultrashort pulses has steadily emerged as a prominent manufacturing technique for producing highly precise holes in microscale range with well-defined edges and minimum heat-affected zone (HAZ) surrounding them. However, ultrashort laser sources are still considered capital intensive and commonly associated with low material removal rates, which results in high operating costs [5]. To satisfy the requirements for high-throughput and enable their broader implementation in industrial applications, significant efforts have been invested towards developing high-average-power ultrashort lasers, i.e. > 100 W. Even though such laser sources offer production upscaling potential, it is really challenging to avoid undesired heat accumulation effects, e.g. surface oxidation and recast/burr formation, accompanying their use [6]. In general, such laser-induced thermal effects are more pronounced at high pulse repetition rates and can have a detrimental impact on the overall drilling efficiency and hole quality, especially in laser percussion drilling of metal

foils. Therefore, effective solutions are required to exploit the aforesaid advances in ultrashort laser technology.

For laser percussion drilling, two methods have been widely promoted to utilise the maximum average power of a typical laser system while mitigating against thermal accumulation of residual heat. The first approach employs laser beam splitting, e.g. diffractive optical elements, to enable parallel laser processing with multiple beamlets on target simultaneously [7-9], whilst the second method uses typically fast beam deflection units, e.g. polygon scanners, together with high repetition rates to move the laser beam across the substrate at very high speeds and deposit a single pulse at each hole location in a series of repeated processing cycles [10, 11]. Nevertheless, these laser drilling strategies involve complex beam delivery setups that hinder their broader adoption on an industrial scale. Thus, burst mode ultrashort laser processing has been proposed as an alternative solution to improve both the process efficiency and heat-related issues by having a better control over the laser energy deposited on the target material. In such laser operating mode, a high energy single ultrashort pulse is divided into a burst of multiple sub-pulses of lower energy closely spaced in time at MHz or GHz level repetition rates. This enables better utilisation of the output laser power by maintaining the incident laser fluence of each sub-pulse at an optimal level. Owing to this unique functionality that this technology offers, extensive research has been conducted to explore the benefits of using MHz or GHz burst mode in laser processing of metallic materials [12-15]. Most of these studies revealed significant improvements in terms of ablation efficiency and surface

quality compared to the standard single-pulse laser mode processing. However, investigations of burst mode laser processing on metals have mainly focused on laser structuring/milling applications so far, whereas there is limited knowledge about its potential in higher aspect ratio laser drilling operations. Specifically, its potential advantages and limitations for high-density percussion laser drilling of metal foils have not been examined.

Therefore, this research reports on throughput upscaling by utilising a 120 W femtosecond diode-pumped solid-state laser in both single-pulse and MHz burst modes for percussion drilling of stainless-steel foils. Herein, the influence of critical laser parameters was investigated in terms of overall process efficiency and quality by evaluating the morphological and dimensional characteristics, i.e. size, HAZ and burr formation, of drilled holes. Lastly, heat accumulation effects induced in MHz burst mode microdrilling of high-density holes were analysed, and then compared with those of nanosecond laser pulses of similar temporal length.

## 2. Material and methods

AISI 304L stainless-steel (SS) foils of 300  $\mu\text{m}$  thickness were used of about  $20 \times 20 \text{ mm}^2$  in size. The substrates were ultrasonically cleaned in ethanol for 30 minutes before and after their laser treatment to remove any possible contamination and residual debris. Laser drilling was performed on a high-power laser micro-machining platform under normal atmospheric conditions, and its main beam delivery sub-system is schematically illustrated in Fig. 1. This workstation integrated an ultrashort laser source (LXR 120-1030, Luxinar) with 800 fs pulse duration at 1030 nm and maximum pulse energy of 120  $\mu\text{J}$  at 1 MHz repetition rate. Circular polarisation was used in all drilling operations. The laser could deliver bursts with up to 172 sub-pulses at an intra-burst repetition rate of 40 MHz, i.e. temporal period of 25 ns between them. The maximum burst energy was 566  $\mu\text{J}$ , and could only be achieved at 200 kHz. The energy distribution across sub-pulses had a descending trend due to amplifier gain saturation. A comparison was made with a 70 W, 1064 nm nanosecond fibre laser (EP-Z G4, SPI/Trumpf) with randomised polarisation, emitting pulses of tunable duration in the range 5 ns – 2  $\mu\text{s}$ .

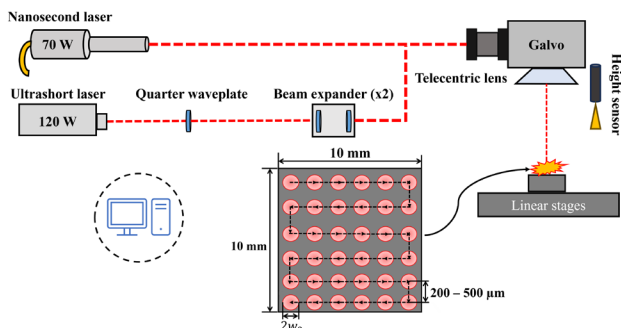


**Fig. 1** Schematic illustration of the laser micro-machining workstation employed to execute the percussion drilling operations.

A galvanometer scanner (excelliSCAN 14, SCANLAB) equipped with a coaxial camera was added in the experimental setup to deflect the laser beam across the SS surface

at high speeds and also monitor the progress of laser drilling. A 163 mm focal length telecentric lens was attached to focus the beam down to a spot size ( $2w_0$ ) of 38  $\mu\text{m}$  and 43  $\mu\text{m}$  at  $1/e^2$  for the nanosecond and femtosecond lasers, respectively. To accurately position the samples at the lens focal plane, three linear (XYZ) motorized stages together a laser triangulation sensor were deployed. Finally, a dedicated CAD/CAM control software (Direct Machining Control) was deployed to control the various laser component technologies and generate the required beam motion trajectories.

Initially, individual test holes were produced on the SS substrates via MHz burst and single-pulse modes to investigate their overall drilling performance. The laser average power, repetition rate, number of pulses/bursts and number of sub-pulses per burst were varied, and their impact on the drill rate, hole dimensions and quality of hole was analysed. To attain reliable and reproducible results, all the drilling operations were carried out in triplets. These sets of holes were then used as reference to evaluate the laser heat accumulation effects induced when drilling high-density holes. Specifically, the high-density drilling operations were performed over a  $10 \times 10 \text{ mm}^2$  surface area on the SS substrates, in which a bidirectional sequential scanning strategy was used to drill holes with pitch distances ranging from 200 to 500  $\mu\text{m}$  as shown in Fig. 1. To initiate heat accumulation between holes and study its effects, the scanner jump speed was varied between 10 and 1600 mm/s. The drilled holes were measured with an optical microscope at five different locations, i.e. on the corners and near the centre of the  $10 \times 10 \text{ mm}^2$  area. Specifically, a surface area of  $3 \times 3 \text{ mm}^2$  containing laser drilled holes was scanned at each of these locations, and then analysed using the technique described in [16]. In this research, only deviations in the hole exit diameter were considered to assess the impact of heat accumulation on the MHz burst mode drilling performance.

## 3. Results and discussion

### 3.1 Single-pulse mode laser drilling

Firstly, we determined the single-shot ablation threshold peak fluence to be 1.9  $\text{J}/\text{cm}^2$  on 300  $\mu\text{m}$  thick SS foils using Liu's method [17] by generating micro-dimples on the SS surface at different laser fluences and measuring their diameters. The multi-pulse ablation threshold fluence was not examined yet.

The minimum number of laser pulses required to perforate the SS substrate i.e. the laser drilling time per hole, was investigated for single-pulse mode percussion drilling. The maximum available pulse energy at 112  $\mu\text{J}$  was used whilst the repetition rate was varied from 50 kHz to 1 MHz. It is evident from Fig. 2(a) that the number of laser pulses needed to perforate the material at fixed pulse energy decreases with increasing repetition rate. The shortest breakthrough drill time of 30  $\mu\text{s}$  was recorded at 1 MHz. The steady decrease in drill time was attributed to residual heat accumulation in the irradiated area by successive laser pulses. This was more pronounced at higher repetition rates as any residual laser heat remaining in the vicinity of the holes could not be removed fast enough before a subsequent laser pulse arrived due to the low thermal conductivity of SS material, which likely led to the ablation threshold

reduction. Such experimental findings are in good agreement with previous studies, in which improved material removal rates were observed when intense laser-induced heat accumulation effects were present [18, 19]. This phenomenon could also explain the fact that a well-rounded exit hole (see inset images in Fig. 2(a)) was only achieved at 1 MHz since the arriving laser fluence at the exit is expected to be higher, having less temperature gradients between consecutive pulses.

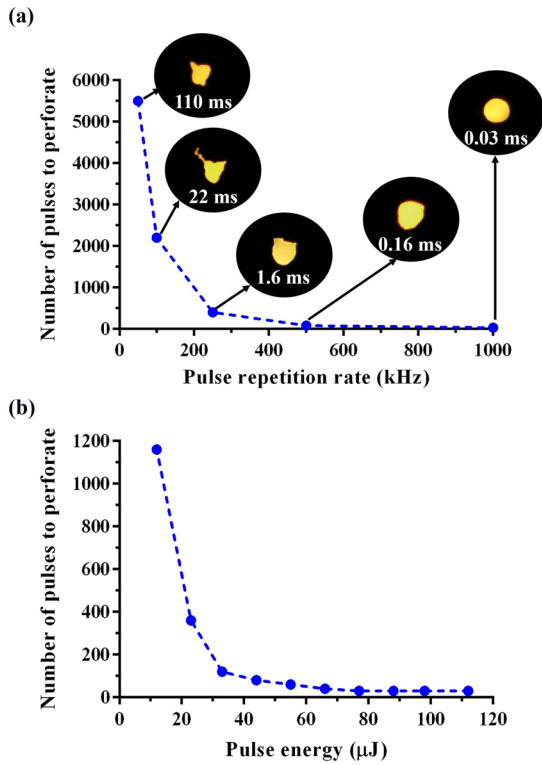


**Fig. 2** The minimum number of pulses required to perforate the SS foils as a function of (a) pulse repetition rate at a fixed pulse energy of 112  $\mu\text{J}$  and (b) pulse energy at a fixed repetition rate of 1 MHz. Insets in (a) show backlit images of the exit holes.

The influence of laser pulse energy on the minimum number of pulses required to penetrate the SS substrates was investigated at a fixed repetition rate of 1 MHz. Fig. 2(b) shows the minimum number of laser pulses required to perforate the foil in percussion with laser pulse energy. For pulse energies below 12  $\mu\text{J}$ , 3000 consecutive incident laser pulses were insufficient to perforate the material. Drilled through holes started to appear by further increasing the pulse energy. In general, higher pulse energy levels resulting in shorter breakthrough times. From 70  $\mu\text{J}$  and beyond up to the maximum available 112  $\mu\text{J}$ , the same number of pulses, i.e. 30, was required to perforate the SS material.

After initially penetrating the SS material, the evolution of hole size with the number of laser pulses was investigated for pulse energies ranging from 33 to 112  $\mu\text{J}$ . The repetition rate was kept constant at 1 MHz. Indicative results on hole size evolution are plotted in Fig. 3 for the maximum available pulse energy of 112  $\mu\text{J}$ . It is apparent that both the entry and exit hole diameters initially increased with the number of incident laser pulses and then reached saturation. Although not shown here, this was also true for all investigated laser pulse energies. Around 500 laser pulses were

required to reach hole size saturation for both entry and exit at the highest pulse energy and 1160 laser pulses at the lowest one.

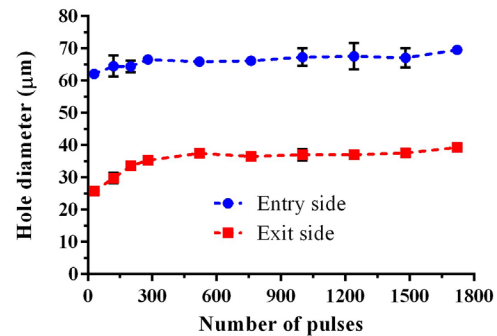


**Fig. 3** The evolution of laser drilled hole size with the number of incident laser pulses for a fixed repetition rate of 1 MHz and pulse energy of 112  $\mu\text{J}$ .

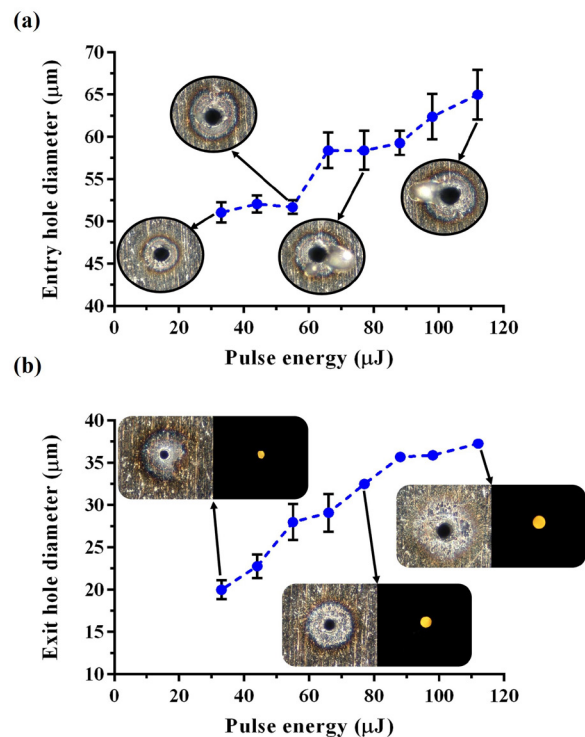


**Fig. 4** (a) Entrance and (b) exit diameters of drilled holes as a function of pulse energy for a fixed repetition rate of 1 MHz and 1160 incident laser pulses.

Lastly, the effect of laser pulse energy on the resulting morphological and dimensional characteristics of drilled through holes was assessed, keeping all other laser processing parameters constant, i.e. repetition rate of 1 MHz, focused spot size and 1160 incident laser pulses on target. As shown in Fig. 4, there is an almost linear relationship between both the entry and exit diameters of through holes with the laser pulse energy. Considering the inset micrographs in this figure, signs of HAZ in the form of surface discoloration/oxidation are observed around both entry and exit sides of the holes for all applied pulse energies. Burr/recast, i.e. molten material ejected and solidified, was also formed around the entrance hole when the pulse energy was higher than 70  $\mu\text{J}$ . Although there is no concrete proof in this work, it is likely that such heat accumulation

effects were initiated by gradual surface temperature rise above 200 °C in a shallow film around the irradiated region during the drilling operation as laser-induced heat was not able to diffuse fast enough away from that region.

From all above results, it is not surprising that increasing both laser pulse energy and repetition rate, i.e. increasing average laser power on target, is essential to scale-up laser percussion drilling speed in single-pulse mode, but this comes at the expense of drilled hole quality.

### 3.2 MHz burst mode laser drilling

We also evaluated MHz burst mode to improve the laser percussion drilling operations at high-average-powers. The maximum output laser power possible from the laser was utilised in these experiments, which corresponds to a burst energy of 566  $\mu\text{J}$  at 200 kHz.

Firstly, the potential of burst mode to speed up drilling rates was investigated. The minimum number of bursts required to perforate the SS material carrying different number of sub-pulses in each burst is presented in Fig. 5(a). Evidently with increasing the number of sub-pulses in a burst, the laser energy of each sub-pulse decreases accordingly. Although the overall laser energy delivered on the SS substrate per burst was the same, the total number of bursts required to drill through gradually decreased with increasing the sub-pulses from 5 to 100. The shortest breakthrough drill time achieved using the MHz burst mode was only 25  $\mu\text{s}$ , which was marginally lower than that achieved with single-pulse mode. Five bursts of 566  $\mu\text{J}$  with 100 sub-pulses each were required to perforate the SS substrate.

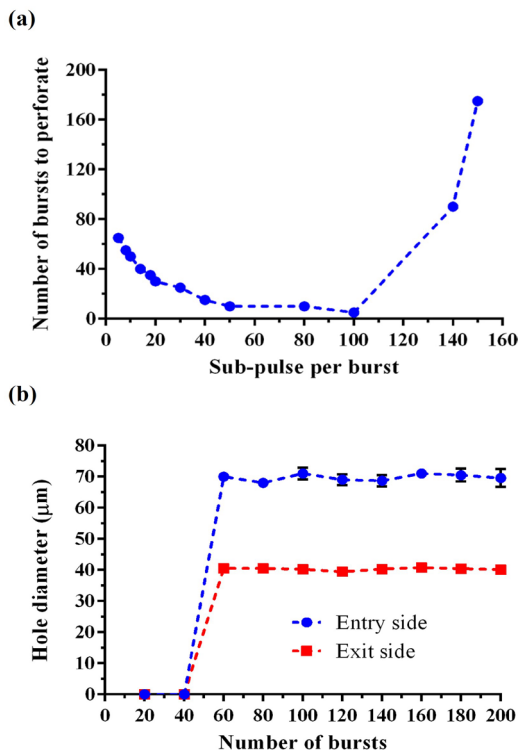


**Fig. 5** MHz burst mode percussion drilling at 566  $\mu\text{J}$  and 200 kHz: (a) the minimum number of laser bursts required to perforate the SS foils with different sub-pulses per burst and (b) hole size as a function of the incident number of laser bursts using 10 sub-pulses in each.

Interestingly, in bursts with more than 20 sub-pulses, the resulting average laser fluence of each sub-pulse is below the nominal ablation threshold determined with single-pulse mode. This would imply that no drilling should be taking place for such bursts. But not only it does, it is also much more efficient to penetrate through the material than laser bursts with higher individual sub-pulse fluence. Based on literature, such improvement in drilling rate has been attributed to photoincubation effects from exposure to the multiple sub-pulses in each burst and associated heat accumulation occurring from their very high intra-burst repetition rate [13, 15]. A reversal in drilling efficiency gains occurs when increasing the number of sub-pulses in each burst beyond 100. In such case, more laser bursts were necessary to drill through holes. For instance, with 140 sub-pulses per burst of only 4  $\mu\text{J}$  each, more than 80 bursts were needed to penetrate through the material. At such long bursts, the fluence of each sub-pulse was significantly low and hence likely insufficient to initiate strong heat accumulation/incubation effects.

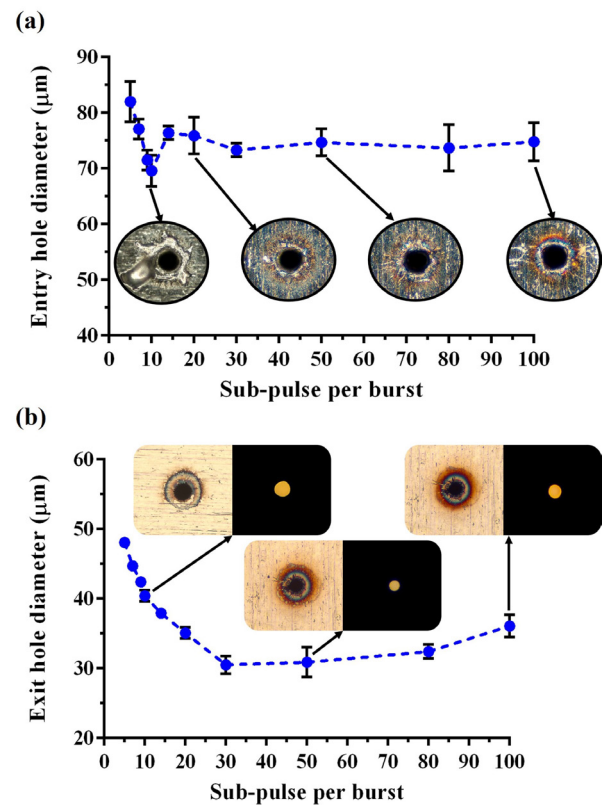


**Fig. 6** Influence of number of sub-pulses within a burst on (a) entry and (b) exit diameter of holes drilled at a fixed repetition rate of 200 kHz and 200 bursts. The insets in (a) and (b) depict optical images of the entry and exit side of holes, respectively.

Furthermore, the evolution of hole size with the number of incident laser bursts was assessed using the maximum available burst energy of 566  $\mu\text{J}$  and 10 sub-pulses in each. As shown in Fig. 5(b), no significant differences were detected in both the entry and exit hole diameters with increasing laser bursts, which contrasts the results obtained in single-pulse laser processing mode. This conveniently implies that an even faster drilling rate can be achieved in MHz burst mode operation since hole size saturation is

reached almost immediately after breaking through the SS material. The effect of the incident number of sub-pulses within a burst on the dimensional and morphological characteristics of holes drilled in SS were also studied. In Fig. 6(a), the entry hole diameter initially decreased linearly with the number of sub-pulses followed by a slight increase and then a plateau. By inspecting the optical images of these holes (see insets in Fig. 6(a)), it was apparent that a ring-like burr was formed around the hole entrance drilled with up to 10 sub-pulses in a burst, which gradually started to recede with increasing their number up to 100. These preliminary experimental findings demonstrate the ability of femtosecond MHz burst mode to control laser heat accumulation and mitigate some of its unwanted side effects, thus minimising the need for laborious post-processing steps to improve hole quality.

In addition, one can see from Fig. 6(b) that the aforesaid laser burst parameter had a stronger impact on the hole exit size. The exit hole diameter initially decreased with the number of sub-pulses per burst and then reached a plateau. This decrease was linear for up to 30 sub-pulses, possibly due to a lower sub-pulse laser fluence. At the same time, laser drilling with a higher number of sub-pulses in a single burst led to brighter surface coloration on the area surrounding the exit hole. Lastly, we report on another important advantage of using burst mode processing in laser percussion drilling operations. Owing to the flexible control of energy deposition offered with this laser output mode, a wide range of hole dimensions can be achieved by simply adjusting the total burst energy and the number of sub-pulses per burst. For instance, exit hole diameters varying from about 10 to 50  $\mu\text{m}$  were drilled on the SS substrates with varying burst energy from 168 to 566  $\mu\text{J}$  and selecting between 5 to 40 sub-pulses as shown in Fig. 7.

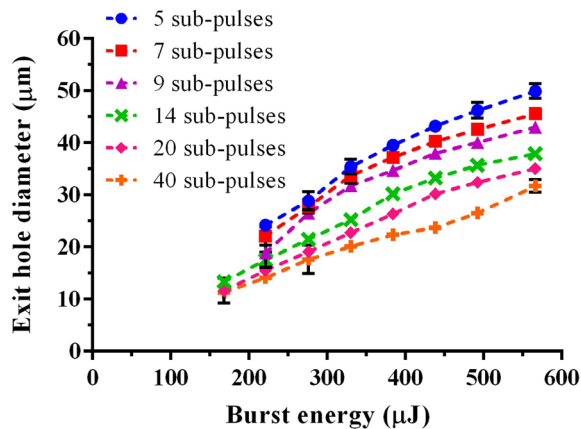


Fig. 7 Exit hole diameter as a function of burst energy for six different sub-pulses per burst.

### 3.3 High-density hole drilling

The capability of MHz laser burst mode to drill high-density holes was investigated over a surface area of  $10 \times 10 \text{ mm}^2$  on the SS samples as this is a common industrial enquiry. By high density we mean holes drilled as close together as possible. As proof of concept, a sequential scanning strategy was employed, meaning each subsequent drilled hole was neighbouring the one drilled immediately next to it. The following fixed laser parameters per hole

location were used: burst energy of 566  $\mu\text{J}$ , 200 laser bursts, repetition rate of 200 kHz and 10 sub-pulses in each burst. Initially, through holes were drilled with a pitch varying from 200 to 500  $\mu\text{m}$ . The impact of pitch distance on the exit hole dimensions was assessed. To prevent any heat transfer between holes at this stage, a time delay of 4 seconds was deliberately introduced between their drilling. This time interval allowed the SS material surrounding the hole to cool back down to room temperature after each hole drilling. As expected, these holes did not exhibit any considerable variations in their exit diameter. This was the case even for those drilled at the tightest examined pitch of 200  $\mu\text{m}$  as shown in Fig. 8.

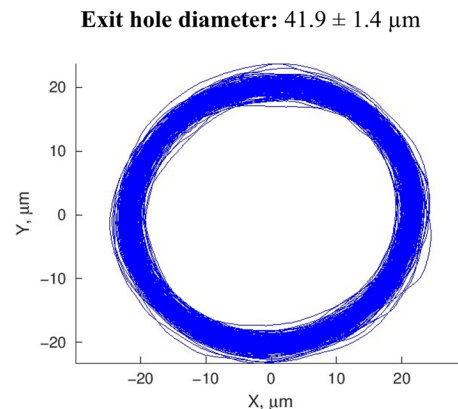


Fig. 8 Overlaid profiles of exit holes drilled at 200  $\mu\text{m}$  pitch in the absence of heat accumulation effects.

Thereafter, the same laser drilling trials were repeated on a fresh area but with increasing galvanometer scanner indexing speeds between holes, i.e. from 10 to 1600 mm/s, and without applying any time delay. That reduced the laser transit time between each hole and could affect the drilling outcome if it was comparable to thermal relaxation time. Indeed, Fig. 9(a) shows that for holes processed at pitch distances higher than 300  $\mu\text{m}$ , the increase in inter-hole indexing speed had a marginal effect on their exit hole sizes. At such pitch distances, there was probably not enough time for any residual heat from neighbouring holes to dissipate and gradually build up ahead of drilling the next one. However, substantial variations were observed in the exit hole diameter at shorter pitch distances below 200  $\mu\text{m}$ . Such holes reached maximum size at indexing speed 400 mm/s, followed by a decrease in size with its further increase. For instance, a deviation of more than 10  $\mu\text{m}$  in average exit diameter was calculated when comparing holes processed at 400 mm/s with reference ones depicted in Fig. 8. Interestingly, a very similar behaviour was observed in our previous results using a nanosecond pulsed laser at its highest output settings, i.e. pulse energy of 1 mJ and repetition rate of 70 kHz, in which undesirable effects of heat accumulation in high-density hole drilling were analysed [20]. The respective results obtained with that laser emitting pulses of 240 ns duration are plotted in Fig. 9(b) for comparison. A close look reveals that these two different laser sources (nanosecond and femtosecond near-infrared) demonstrate an almost identical drilling behaviour in terms of hole uniformity. Thus, despite common belief, it is apparent that undesired heat accumulation effects are

present in high-density drilling of SS even for femtosecond lasers operating in burst mode.

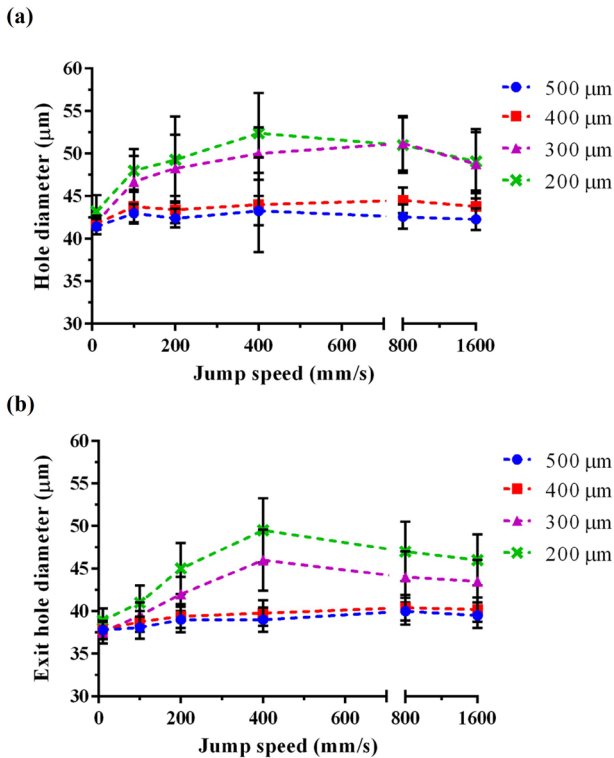


Fig. 9 The influence of laser jump speed as a function of exit diameter of holes drilled at different pitch distances with (a) a femtosecond pulsed laser operating in burst mode and (b) a nanosecond pulsed laser.

#### 4. Conclusions

The potential of MHz femtosecond laser burst mode was investigated in this paper to improve laser percussion drilling of SS foils while utilising fully the 120 W output power of a 800 fs near-infrared ultrashort laser, and its performance was compared with single-pulse output. The influence of critical laser processing parameters in both regimes was investigated for maximum drilling efficiency and best hole quality by evaluating the dimensional and morphological characteristics of drilled holes. High-average-power single-pulse laser mode (112 W at 1 MHz) could significantly increase drilling throughput comparing to lower power laser sources. However, laser processing with these settings led to poor hole quality due to intense heat accumulation. On the contrary, MHz burst output of the same average power exhibited clear advantages in terms of drilling efficiency and overall hole quality. This mode enabled faster drilling rates without compromising hole quality by carefully optimising the number of sub-pulses in the burst. The shortest drill time achieved through 300 μm thick stainless steel was 25 μs per hole, attained with 100 sub-pulses in a 566 μJ burst. Consequently, MHz burst mode can be an effective solution to exploit the continuous increase in high-average-power of industrial femtosecond lasers for upscaling drilling processes. However, its

performance in high-density hole drilling was unremarkable, producing very similar results to that of mere nanosecond fibre lasers operating with pulses of similar total temporal length to the burst duration. Thus, MHz burst mode as a stand-alone technology is not sufficient to suppress/mitigate the undesired heat accumulation effects present at high processing speeds in such operations.

#### Acknowledgments

We would like to acknowledge the support from Physik Instrumente (PI) GmbH and Luxinar Ltd in this research.

#### References

- [1] K. P. Maity and R. K. Singh: *Int. J. Adv. Manuf. Technol.*, 61, (2012) 1221.
- [2] M. Putzer, N. Ackerl, and K. Wegener: *Int. J. Adv. Manuf. Technol.*, 117, (2021) 2445.
- [3] M. Hasan, J. Zhao, and Z. Jiang: *J. Manuf. Process.*, 29, (2017) 343.
- [4] A. Piqué, R. C. Y. Auyeung, H. Kim, N. A. Charipar, and S. A. Mathews: *J. Phys. D: Appl. Phys.*, 49, (2016) 223001.
- [5] T. Karkantonis, A. Gaddam, X. Tao, T. L. See, and S. Dimov: *Surf. Interfaces*, 31, (2022) 102096.
- [6] D. Brinkmeier, D. Holder, A. Loescher, C. Röcker, D. J. Förster, V. Onuseit, R. Weber, M. A. Ahmed, and T. Graf: *Appl. Phys. A*, 128, (2021) 35.
- [7] J. Finger and M. Hesker: *J. Phys. Photonics*, 3, (2021) 021004.
- [8] E. Biver, J. Dupuy, Y. Hernandez, A. Henrottin, J. Pouysegur, and R. Ocaña: *J. Laser Micro Nanoeng.*, 18, (2023) 36.
- [9] C. Lutz, J. Helm, K. Tschirpke, C. Esen, and R. Hellmann: *Materials*, 16, (2023) 5775.
- [10] F. Roessler and A. Streek: *Adv. Opt. Technol.*, 10, (2021) 297.
- [11] F. Rößler, M. Müller, and A. Streek: *J. Laser Micro Nanoeng.*, 15, (2020) 220.
- [12] A. Žemaitis, M. Gaidys, P. Gečys, M. Barkauskas, and M. Gedvilas: *Opt. Express*, 29, (2021) 7641.
- [13] H. Le, T. Karkantonis, V. Nasrollahi, P. Penchev, and S. Dimov: *Appl. Phys. A*, 128, (2022) 711.
- [14] P. Lickschat, A. Demba, and S. Weissmantel: *Appl. Phys. A*, 123, (2017) 137.
- [15] P. Lickschat, D. Metzner, and S. Weißmantel: *J. Laser Appl.*, 33, (2021) 022005.
- [16] J. Martan, D. Moskal, L. Smeták, and M. Honner: *Micromachines*, 11, (2020) 520.
- [17] J. M. Liu: *Opt. Lett.*, 7, (1982) 196.
- [18] J. Martan, L. Prokešová, D. Moskal, B. C. Ferreira de Faria, M. Honner, and V. Lang: *Int. J. Heat Mass Transf.*, 168, (2021) 120866.
- [19] D. Franz, T. Häfner, T. Kunz, G. Roth, S. Rung, C. Esen, and R. Hellmann: *Materials*, 15, (2022) 3932.
- [20] T. Karkantonis, E. Pelletier, T. Barnard, S. Tuohy, and D. Karnakis: *Proc. LIM*, (2023) 1.

(Received: July 9, 2024, Accepted: December 1, 2024)